Scientific Research Publishing

Open Journal of Applied Sciences, 2016, 6, 796-813
http://www.scirp.org/journal/ojapps
ISSN Online: 2165-3925
ISSN Print: 2165-3917

Structural Morphological and Dielectric Properties of $Pb_{1-x}Ni_xTiO_3$ Doped with Ni

A. Tawfik[1], O. M. Hemeda[1], D. M. Hemeda[1], M. Barakat[1], R. Shady[1,2*]

[1]Faculty of Science Physics Department, Tanta University, Tanta, Egypt
[2]Oklat Al-Skoor Fac. of Science & Arts Physics Department, Qassim University, Qassim, Saudi Arabia
Email: omhemeda@yahoo.com, *rehamshadi81@gmail.com

How to cite this paper: Tawfik, A., Hemeda, O.M., Hemeda, D.M., Barakat, M. and Shady, R. (2016) Structural Morphological and Dielectric Properties of $Pb_{1-x}Ni_xTiO_3$ Doped with Ni. *Open Journal of Applied Sciences*, **6**, 796-813.
http://dx.doi.org/10.4236/ojapps.2016.611070

Received: September 12, 2016
Accepted: October 28, 2016
Published: October 31, 2016

Copyright © 2016 by authors and Scientific Research Publishing Inc.
This work is licensed under the Creative Commons Attribution International License (CC BY 4.0).
http://creativecommons.org/licenses/by/4.0/

Open Access

Abstract

In this paper, we have reported a conformable $PbTiO_3$ ceramics doped with Ni by standard double sintering technique as well as chemical co-precipitation method which were successfully synthesized by means of carefully controlled processing parameters. Single phase formation was confirmed through X-Ray Diffraction (XRD) analysis, IR spectroscopy, SEM micrograph and TEM images. Discussion and comparison between both preparation methods were made on the basis of observed results. The tetragonality c/a decreased from 1.049 to 1.0276 for ceramic samples and decreased from 1.06519 to 1.0365 for co-precipitation samples by increasing Ni content. TEM images show small ferroelectric domains of about 3 to 14 nm for the co-precipitation sample and 26 to 48 nm for the ceramic samples. The SEM of co-precipitation samples shows that the microstructure is very dense. The behavior of ε identifies that our samples are nonrelaxor. Increasing the Ni concentration increases the value of dielectric constant and the T_c is shifted to lower temperature.

Keywords

Lead Titanate, Co-Precipitation Method, Dielectric Constant, Transmission Electron Microscope

1. Introduction

Lead titanate, $PbTiO_3$ ceramic, is a powerful piezoelectric material for high temperature and high frequency applications such as infrared sensors and capacitors. It is very difficult to obtain a pure and dense $PbTiO_3$ phase at a maximum c/a ratio. The influences of doping Ni, Nb and Mn on structural electrical and electromechanical properties of lead titanate were investigated. The anisotropy decreases with increasing amount of dopants [1].

The small amount of Ca changes the electrical conductivity and the transition temperature T_c of ferroelectric phase. The XRD and SEM analysis shows the increase of grain and particle size with the increase of Ca. The dc conductivity of lead titanate doped with Ca is influenced by Ca content at room temperature and near transition temperature. The T_c temperature shifts to lower values by increasing Ca addition [2].

The electrical and microstructure properties of piezoelectric ceramic system (Bi-YbO_3-$PbTiO_3$)-$(PbZnNb)O_3$ were reported. The system had a perovskite structure with a tetragonal phase by increasing PZN, the tetragonality (c/a) decreased the mechanical coupling factor and piezoelectric properties of the samples were improved, which might be attributed to the improved density structural stability and homogeneity [3].

A ternary system of PNZT has been prepared by conventional mixed oxide. The formation of the perovskite phase is established by X-ray diffraction analysis; SEM confirms what we found by X-ray analysis. Dielectric properties like dielectric constant and dielectric loss (ε_0 and $\tan\delta$) indicate poly-dispersive nature of the material. The temperature dependent dielectric constant (ε_0) curve indicates relaxor behavior with two dielectric anomalies. The poly-dispersive nature of the material is analyzed by Cole-Cole plots. The activation energy follows the Arrhenius law and is found to decrease with increasing frequency for each composition. The frequency dependence of ac conductivity follows the universal power law. The ac conductivity analysis suggests that hopping of charge carriers among the localized sites is responsible for electrical conduction. The ferroelectric studies reveal that these ternary systems are soft ferroelectric [4].

The objective of the present work is to improve the physical and piezoelectric properties of $PbTiO_3$ by the addition of Ni ions and to prepare the $PbTiO_3$ by different methods to make a comparison between the ceramics and co-precipitation samples.

2. Experimental Procedure

First series perovskite $Pb_{1-x}Ni_xTiO_3$, x = (0.0, 0.1, 0.2, 0.3, 0.4 and 0.5) has been prepared using a conventional ceramic process. The oxides were exposed to 800˚C as presintered temperature. The crushed mass was grinded and pressed as disks at 5000 kg /cm^2 and sintered at 1200˚C for 2 hours then left to be cooled gradually with the rate 50˚C/hr. The co-precipitation procedure were used to prepare the other series of $Pb_{1-x}Ni_xTiO_3$ (x = 0.0, 0.1, 0.2, 0.3, 0.4 and 0.5). The chemical reagents were Titanium chloride ($TiCl_3{\cdot}15H_2O$), Nickel (II) chloride ($NiCl_2{\cdot}6H_2O$), Lead chloride ($PbCl_2$) and sodium hydroxide (NaOH). All the chemical reagents were dissolved into 200 ml of distilled water. After mixing and stirring solutions for 6 hours, chemical precipitation was achieved at room temperature vigorous stirring by adding of NaOH solution gradually. The reaction system was kept at 80˚C for 2 hours and PH solution ±12. After the system cooled to room temperature, the precipitates were washed with distilled water until PH-7. Finally the samples dried in oven at 200˚C for several hours and sintered at 1000˚C for 2 hours then left to be cooled gradually with the rate 50˚C/hr.

The samples were examined by x-ray diffraction using a Philips model (PW-1729) diffractometer. IR spectra for the prepared samples were carried out at room tempera-

ture using the Perkin-Elmer-1430 recording infrared spectrophotometer in the range from 200 cm^{-1} to 5000 cm^{-1}. As for the Scanning Electron Microscope of samples, we used SEM Model Quanta 250 FEG (Field Emission Gun) attached with EDX Unit (Energy Dispersive X-ray) Analyses. We used TEM model (Transmission Electron Microscope JEOL-100SX) and HRTEM model (High Resolution Transmission Electron Microscope JEOL EM 2-100). The dielectric measurements were performed using RLC bridge type 815 B. The prepared tablets with silver electrodes were heated with heating rate 4˚C /min; the temperature was controlled by a thermocouple contacting the samples holder near where the sample was situated.

3. Results and Discussion

3.1. X-Ray Diffraction Pattern

The XRD patterns for ceramic and co-precipitation samples of $Pb_{1-x}Ni_xTiO_3$ which (x = 0.0, 0.1, 0.2, 0.3, 0.4, 0.5) are shown in **Figure 1** and **Figure 2** show a well resolved peaks. The values of the full width at half maximum intensity indicate that the polycrystallite has nano sites. This result confirms that the Ni ions occupied the Pb ions site with smaller ionic radius. The reduced c/a ratio suggests that the samples have perovskite phase with tetragonal structure with improved mechanical stability [5] [6].

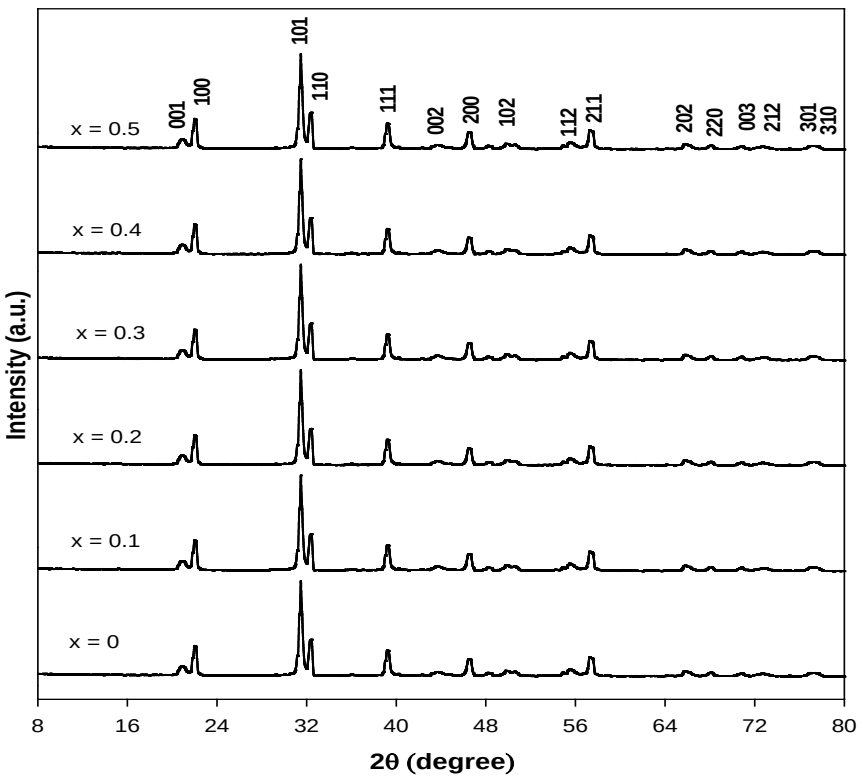

Figure 1. X-ray diffraction patterns of "$Pb_{1-x}Ni_xTiO_3$" system for different Ni content for ceramic method.

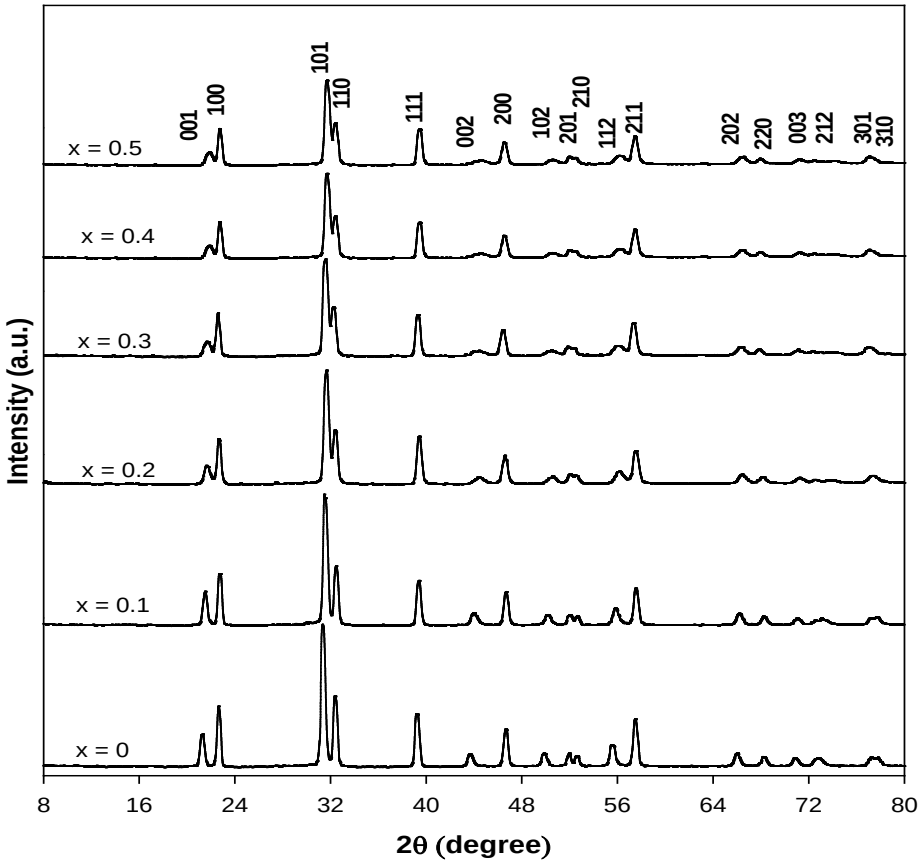

Figure 2. X-ray diffraction patterns of $Pb_{1-x}Ni_xTiO_3$ system for different Ni content for co-precipitation method.

The patterns correspond well to $PbTiO_3$ phase with a typical tetragonal symmetry showing splitted (001/100), (101/110), (002/200) and (112/211) peaks. When Ni content increases, no change for the patterns is observed, whereas the other phases of Ni previously mentioned and PbO disappeared with increasing Ni content and the two peaks in each group of the tetragonal phase patterns approached to each other, indicating decrease in tetragonality. This phenomenon is observed from XRD patterns from the decreasing of the ratio c/a. The appearance of pre-mentioned diffraction peaks demonstrates that the perovskite nano crystallites of $PbTiO_3$ can be formed successfully at 600˚C [6].With increasing Ni content the tetragonality c/a decrease from 1.049 to 1.0276 for ceramic samples and decrease from 1.06519 to 1.0365 for co-precipitation samples. The lattice deformation has high a tetragonality which is a very important factor for piezoelectric performance [7].

The XRD pattern prove that a single which tetragonal phase was obtained for all compositions with different Ni content with a = 4˚A, c = 3.875˚A and c/a = 0.96875, the crystallite size was determined from the line width using Scherer's equation. It is noticed that the samples with low value line width has higher crystallite size as given in **Table 1**. There is a correlation between line width and crystallite size as shown in **Figure 3** between crystallite diameter and $h_{1/2}$. This result is consistent with the correlation

Table 1. Delta theta for the most characteristic tetragonal peaks grain size for ceramic method and co-precipitation method.

Co-precipitation samples				
X	(001/100)	(101/110)	(002/200)	(112/211)
0.0	1.4	0.98	2.96	1.89
0.1	1.26	0.88	2.3	1.7
0.2	1.22	0.72	2.33	1.66
0.3	1.04	0.69	2.16	1.49
0.4	0.93	0.66	2.3	1.41
0.5	0.43	0.34	2.14	1.28
Ceramic samples				
X	(001/100)	(101/110)	(002/200)	(112/211)
0.0	1.34	0.98	2.94	1.87
0.1	1.26	0.87	2.31	1.71
0.2	1.21	0.71	2.34	1.64
0.3	1.02	0.67	2.18	1.49
0.4	0.91	0.64	2.35	1.4
0.5	0.42	0.31	2.15	1.26

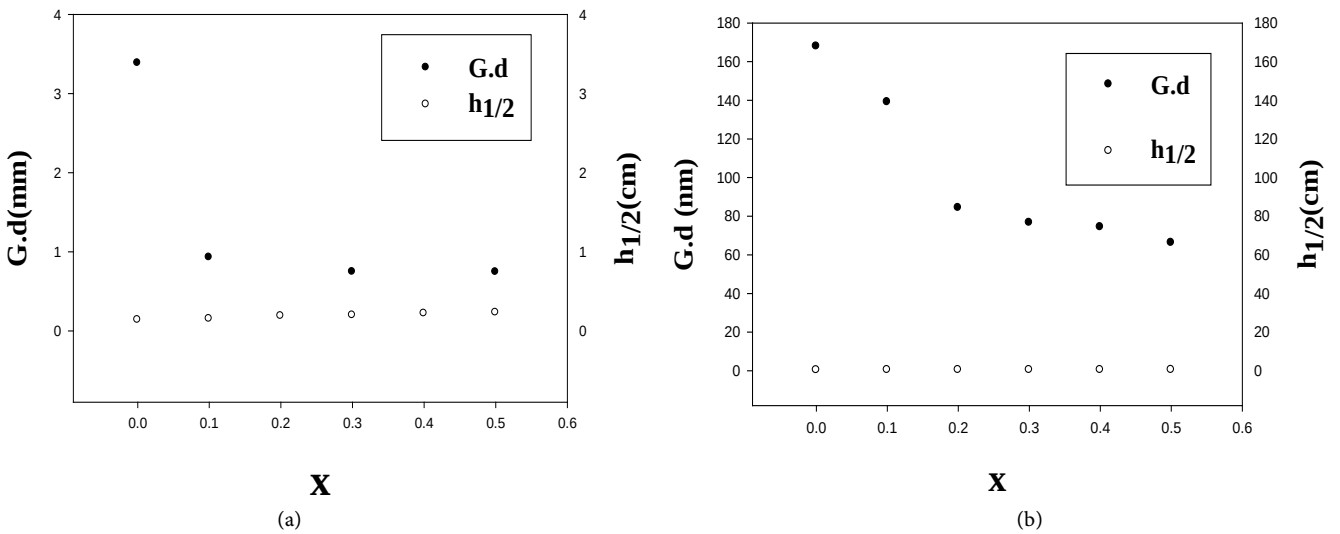

Figure 3. Crystallite size of "$Pb_{1-x}Ni_xTiO_3$" system and $h_{1/2}$ vs. for different Ni content for (a) ceramic and (b) co-precipitation methods.

between the crystallite size and the peak width which widely discussed and reported on PT ceramics [8] [9] and Barium Titanate ceramics [10] [11].

The influence of Ni content on the lattice constant of the prepared materials is shown in **Figure 4**. The lattice constant (a) shows slight increase by 0.72% while the constant (c) decrease by 13.8% for ceramic samples. The lattice constant (a) shows slight increase by 0.61% while the constant (c) decrease by 10.78% for the co-precipitation samples.

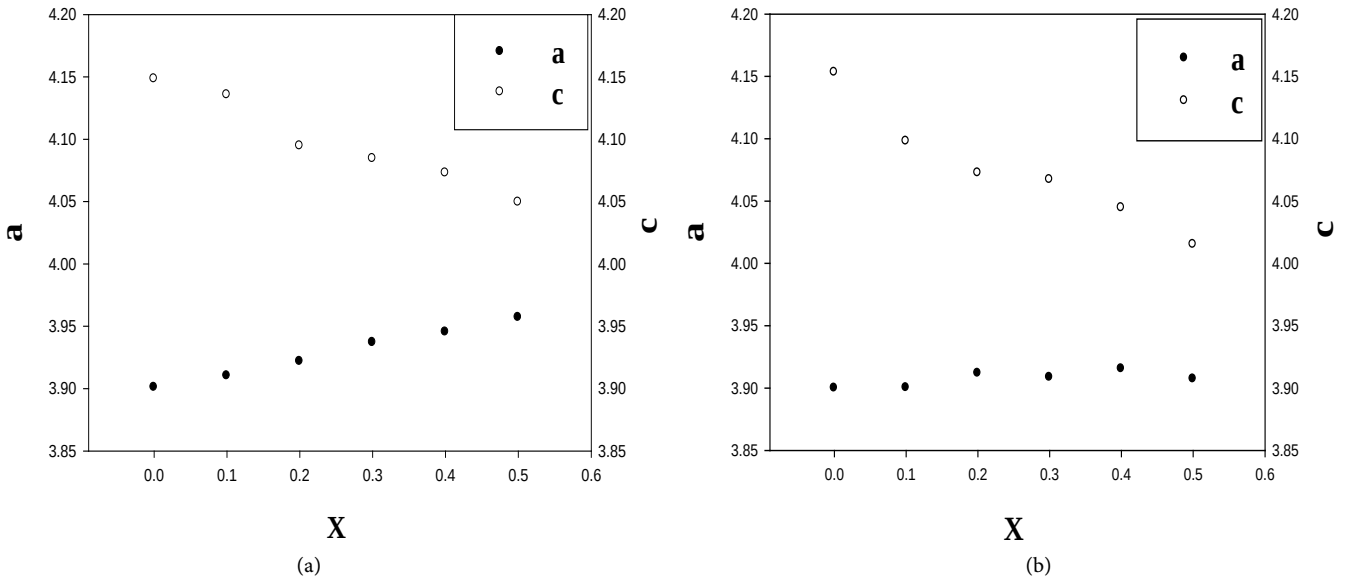

Figure 4. Lattice parameters of $Pb_{1-x}Ni_xTiO_3$ system vs. different ratios of Ni content for (a) co-precipitation (b) ceramic.

The variation of lattice parameter (a) and (c) by increasing Ni content has low values for co-precipitation sample than the ceramic sample. Although the ionic radius of Ni^{2+} is smaller than the Pb^{2+} ionic radius the lattice parameter (a) increase by increasing Ni concentration which is related to the increase of internal strain which cause the lattice to expand in the (a) direction. The decrease of the lattice parameter (c) by increasing Ni content may be due to the low value of the Ni^{2+} ionic radius compared with ionic radius of Pb^{2+}. **Figure 5** also shows decrease of c/a ratio which means that the tetragonality feature of the samples decreases by increasing Ni content. Characteristic peak of around $2\theta = 31.46^\circ$ and the splitted peaks (001/100) indicate the presence of tetragonal phase [12].

Figure 6 shows the porosity of the samples. From the figure it is shown that the samples prepared by co-precipitation have small porosity than ceramic samples and the porosity increased noticeably for increasing Ni contents.

The $PbTiO_3$ doped with Ni are exposed to annealing process at 600˚C, 800˚C and 1000˚C for 2hours to ensure complete crystallization and remove of any foreign phases.

Figure 7 shows the XRD patterns of samples $Pb_{1-x}Ni_xTiO_3$ (x = 0.0, 0.1, 0.2, 0.3, 0.4, 0.5) annealed at 600˚C, 800˚C and 1000˚C Show an increase in the peak intensity by increasing annealing temperature up to 1000˚C. The calculated values of crystallite size for each composition at different annealing temperature were calculated using Scherer's equation. It is noticed that the crystallite size for each composition increases by increasing annealing temperature as given in **Table 2**. In comparison small crystallite size is observed for $PbTiO_3$ doped with Ni powder prepared by co-precipitation method. The crystallite size for co-precipitation samples still in the nano range after annealing at 1000˚C. It is noticed that the diffraction peak at $2\theta = 30^\circ$ belong to precursor. Raw materials disappeared at higher annealing temperature due to the complete formation of $Pb_{1-x}Ni_xTiO_3$.

Table 2. Crystallite size of "$Pb_{1-x}Ni_xTiO_3$" system at different annealing temperature vs. Ni content x for co-precipitation samples.

X	Particle size (nm)		
	600˚C	800˚C	1000˚C
0.0	25.561	21.266	28.417
0.1	15.214	20.835	27.044
0.2	19.413	16.547	20.478
0.3	23.538	19.111	20.435
0.4	25.096	17.712	18.905
0.5	20.442	17.708	18.649

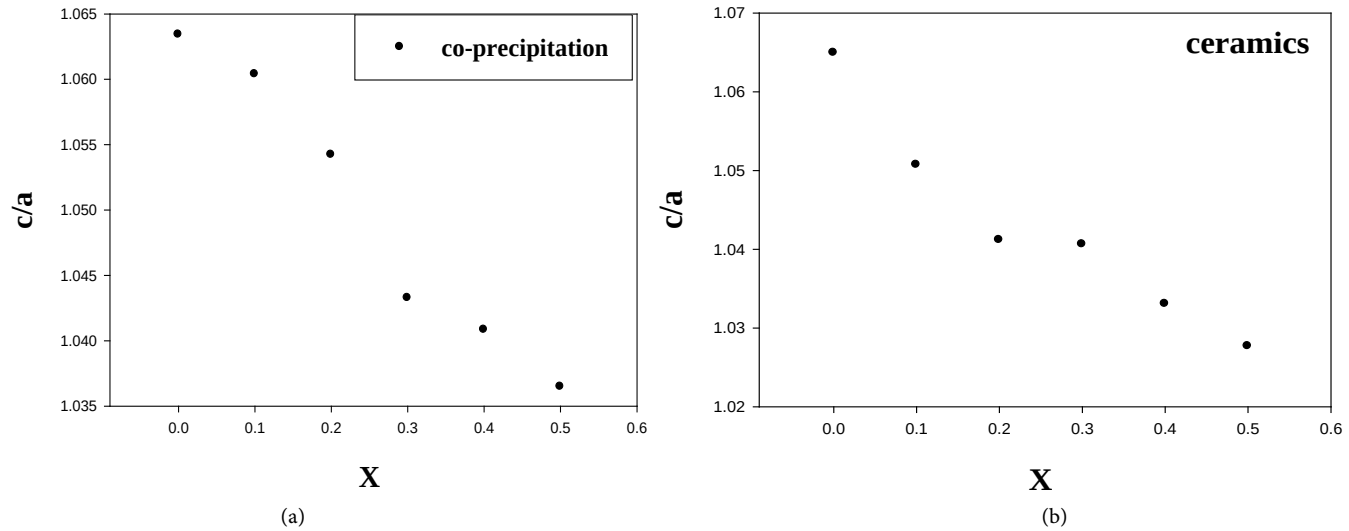

(a) (b)

Figure 5. The ratio c/a, of "$Pb_{1-x}Ni_xTiO_3$" system vs. different ratios of Ni content (x).

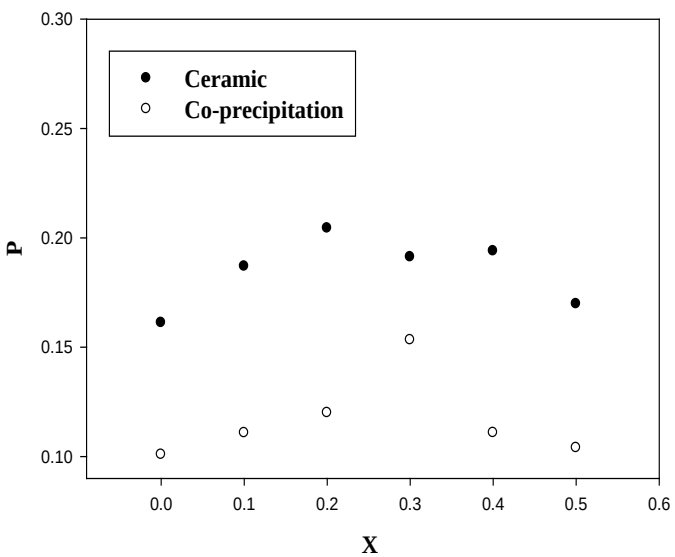

Figure 6. Porosity for "$Pb_{1-x}Ni_xTiO_3$" samples.

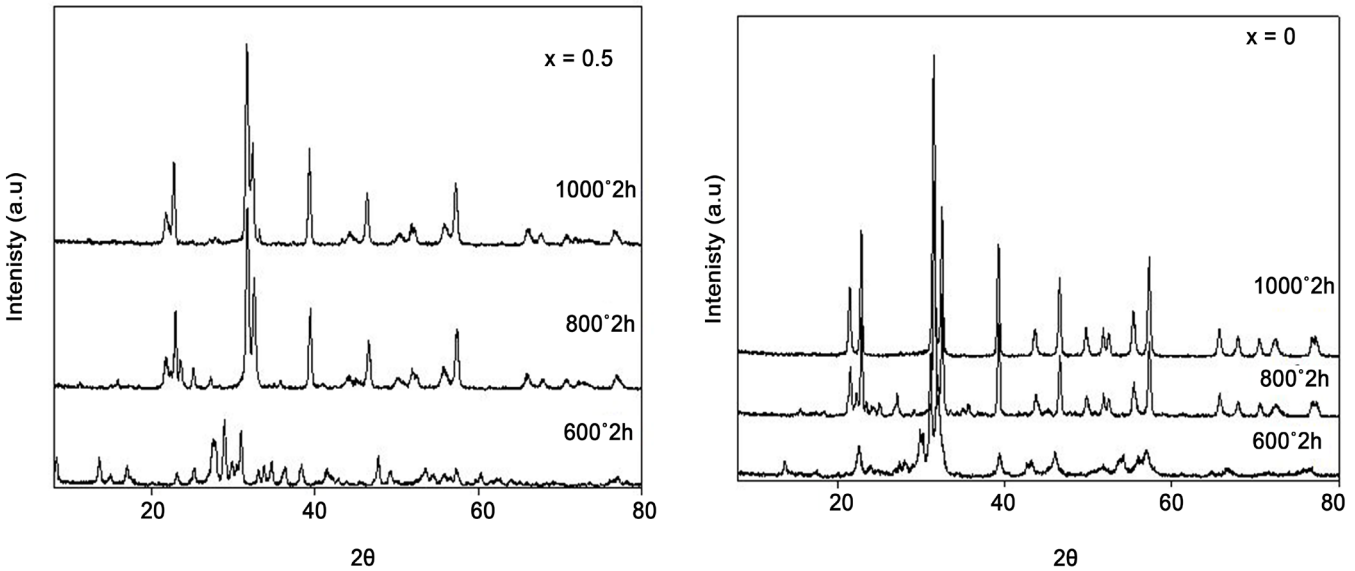

Figure 7. XRD patterns for $Pb_{1-x}Ni_xTiO_3$ system vs. different ratios of Ni content (x) for co-precipitation method at different annealing temperature.

Table 3. Crystallite size of $Pb_{1-x}Ni_xTiO_3$ system at different Ni content for samples prepared.

Co-precipitation	x-ray	28.417	27.044	20.478	20.435	18.905	18.649
	TEM	14.47	13.395	11.56	7.835	4.67	3.244
Ceramics	x-ray	60.356	55.337	44.274	42.170	37.959	35.920
	TEM	48.966	--------	--------	-------	--------	25.629

From Table 3 it is evident that the average crystallite size of the samples prepared by co-precipitation method smaller than that of prepared by ceramic method. The crystallite size derived from XRD has higher value than that derived from TEM since. The XRD is a bulk technical and the crystallites lower than 20 nm are too low to be detected carefully by X-ray.

3.2. Infrared Absorption Spectra

IR spectra carried out in lead titanate doped with Ni prepared by both ceramic and co-precipitation methods are shown in Figure 8(a) and Figure 8(b). The IR spectra showed two vibrational absorption bands one at 377 cm^{-1} and the other at 573 cm^{-1}, another two vibrational peaks appear at 1400 and 1600 for co-precipitation samples and ceramic samples. Additional peak appears at1385 for ceramic sample. The first two peaks around 377 to 573 cm^{-1} are due to metal oxide binding [13].

The wide band appearing at 377, 573 cm^{-1} corresponds to vibrational frequency of Ni-O bond at tetrahedral and octahedral coordination. We can say that the peak appeared around 1400 - 1600 is attributed to the symmetrical H-O-H and as symmetrical H-O-H bond vibration these results are confirmed with the pervious reported data [14]. The presence of the absorption bands in the far infrared region confirms the formation of $Pb_{1-x}Ni_xTiO_3$ structure.

The absorption peak at 500 (υ2) which due to M-O bond shifted to lower frequency from 573 to 553 cm^{-1} which confirming the formation of more perovskite phase at higher Ni concentration. The band near 573 cm^{-1} is associated to octahedral bond and indicates the formation of a perovskite phase.

In conclusion the studies of IR spectroscopy confirm the formation of a perovskite structure.

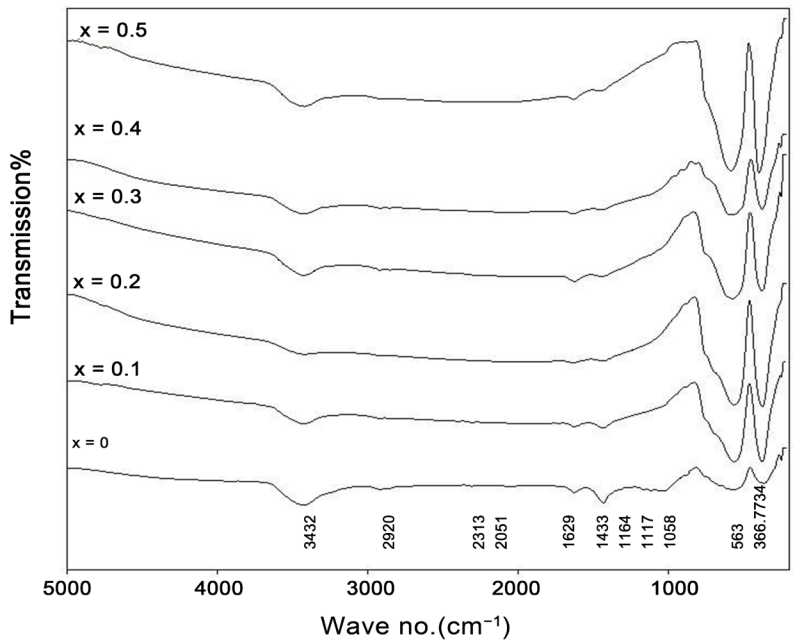

(a)

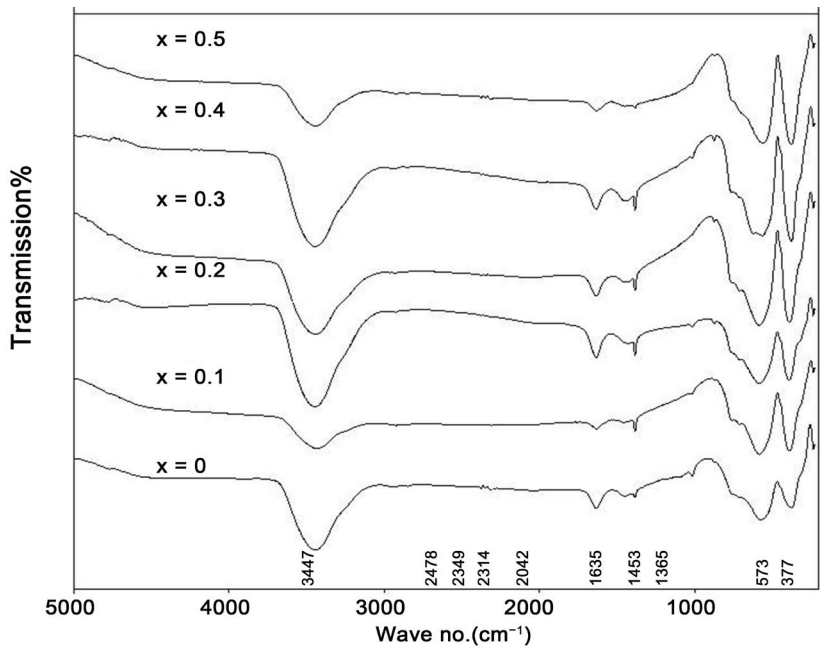

(b)

Figure 8. IR for $Pb_{1-x}Ni_xTiO_3$ (a) co-precipitation samples (b) ceramic samples.

3.3. Scan Electron Microscope (SEM)

Figure 9(a) and Figure 9(b) show SEM micrograph of $PbTiO_3$ doped with Ni content. The micrograph show good densification and homogenous grain size. Some degree of porosity is clearly seen in ceramic samples micrograph where the porosity is very small for the micrograph of co-precipitation samples. The $PbTiO_3$ powder derived from ceramic method consists of particles with size ranged from 3.3 to 0.7 μm. In comparison small particle size is observed for $PbTiO_3$ doped with Ni powder prepared by co-precipitation method. There is correlation between the grain size and the density. The larger grain size has lower density makes density for samples prepared by co-precipitation method higher than that prepared by ceramic method, So the high value of grain size leads to the decrease in density. The density for both samples decrease by increasing Ni content due to the lower atomic weight of Ni compared with Pb. The SEM micrograph for co-precipitation samples have very smaller grain size, grain appearance and regular grain morphology than the SEM for ceramic samples [15]. The grain size was obtained from SEM micrograph which is given in Table 4. The Ni ions can concentrate near the grain boundaries and reduce their mobility so they are considered to be as grain growth inhibitor [16]. The SEM morphology of all samples indicated spherical and tetragonal shape of the grains and that the tetragonality appeared clearly in the co-precipitation samples. Using the line intercept method the average grain size of the samples was determined.

Correlating the micrometer grain size reviled by SEM with the nanometer size of the ferroelectric domain determined by XRD and TEM images one can conclude that ceramic grains have multi domain structure [1].

3.4. Transmission Electron Microscopy (TEM)

The $Pb_{1-x}Ni_xTiO_3$ powder for ceramic and co-precipitation samples treated at 1200˚C and 1000˚C respectively were subjected to TEM microstructure analysis to determine the average particle size. Figure 10(a) and Figure 10(b) show TEM images of the $PbTiO_3$ doped with Ni prepared by ceramic and co-precipitation method. This image reviles that the nanoparticle were not agglomerated for all location of the images with an average particle size ranged from 14.47 to 3.244 nm for co-precipitation samples. There is some agglomeration appears for ceramic sample at some location. Also TEM images show small ferroelectric domains of about 3 to 14 nm for the co-precipitation sample and 26 to 48 nm for the ceramic samples as given in Table 3. Figure 10(a) and Figure 10(b) show spherical and tetragonal crystallites for $PbTiO_3$ phase.

Table 4. Grain size of $Pb_{1-x}Ni_xTiO_3$ system at different temperature for co-precipitation method vs. Ni content.

Samples	X	0.0	0.1	0.2	0.3	0.4	0.5
Co-precipitation at 1000˚C	Gd (nm)	167.76	139	82.26	76.56	74.306	66.22
Ceramics at 1200˚C	Gd (μm)	3.3794	0.9237	------	0.7428	----	0.740057

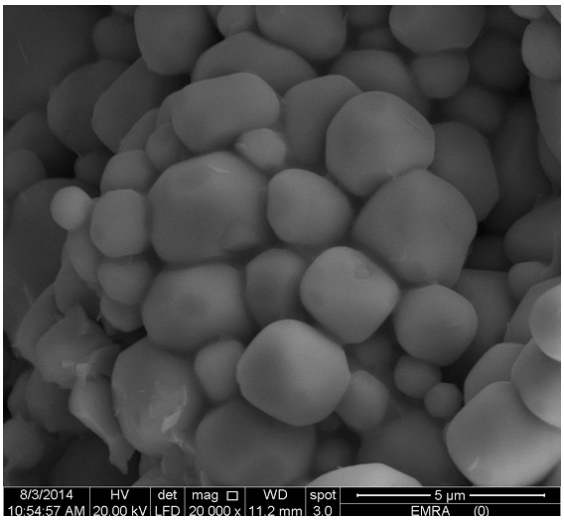

x = 0

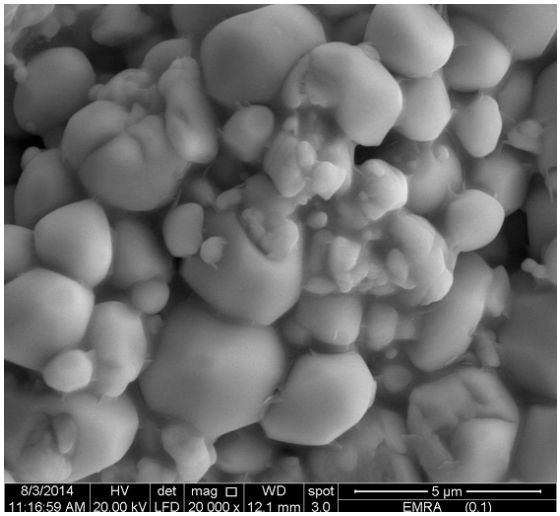

x = 0.1

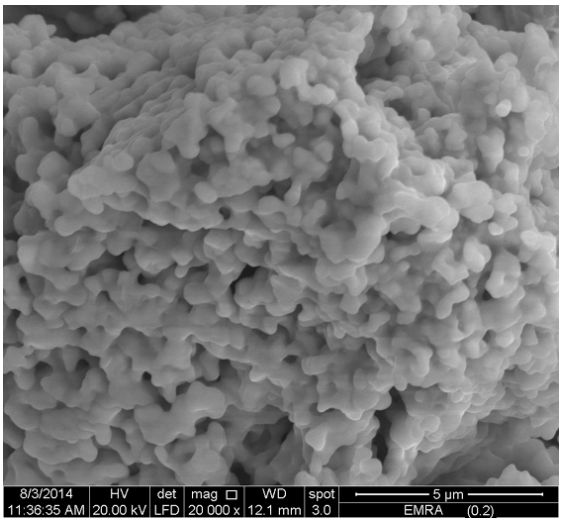

x = 0.2

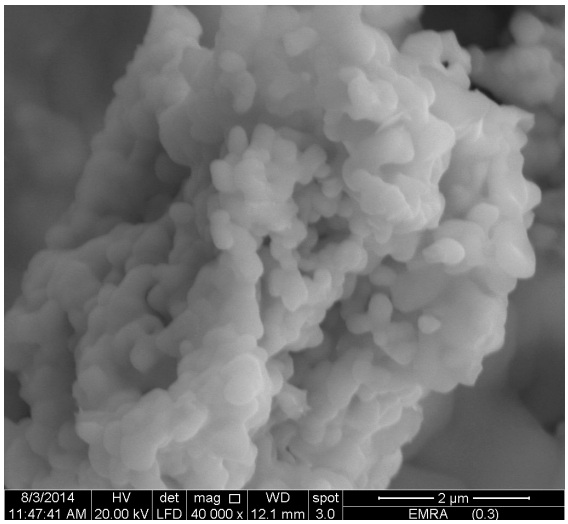

x = 0.3

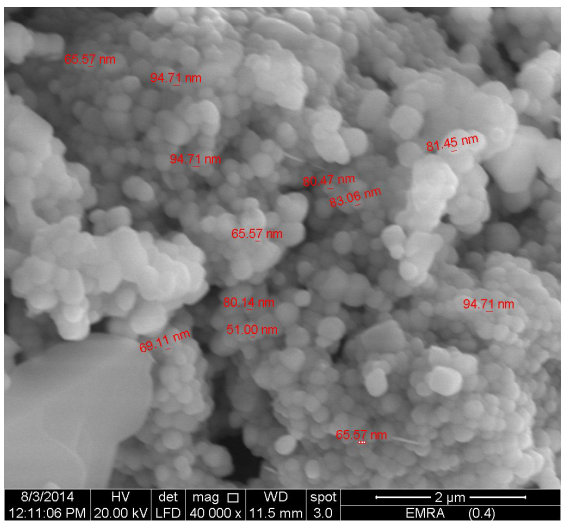

x = 0.4

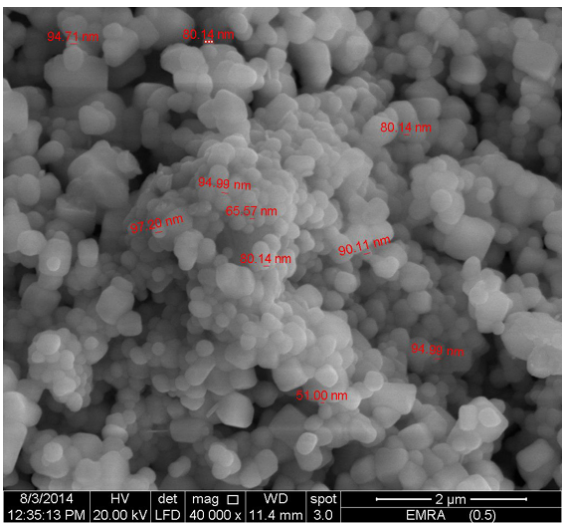

x = 0.5

(a)

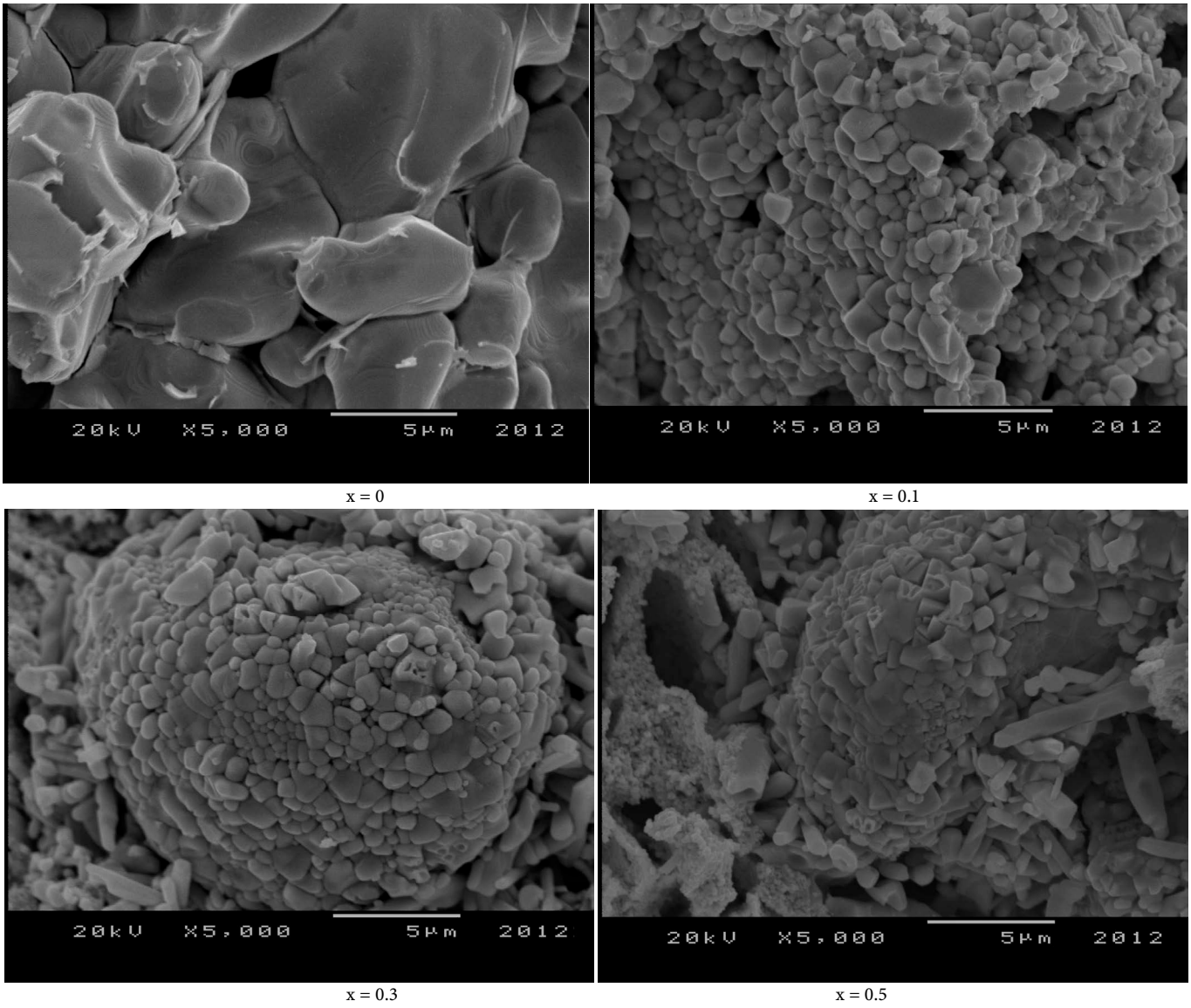

x = 0 x = 0.1

x = 0.3 x = 0.5

(b)

Figure 9. SEM for $Pb_{1-x}Ni_xTiO_3$ (a) co-precipitation samples (b) ceramic samples.

The crystallite size derived from XRD has higher value than that derived from TEM since. The XRD is a bulk technical and the crystallites lower than 20 nm are too low to be detected carefully by X-ray. For the sample x = 0.5 the identification of d spacing d = 0.13nm suggest the tetragonal crystallite as shown in **Figure11** corresponding to 212 plane of $PbTiO_3$ phase [17]. This demonstrates that the nanocrystalite of perovskite $PbTiO_3$ phase was successfully formed by the co-precipitation method.

3.5. Dielectric Constant (ε)

Figure 12 shows the temperature dependence of dielectric constant (ε) at 1 kHz and 10 kHz for both samples prepared by co-precipitation and ceramic methods.

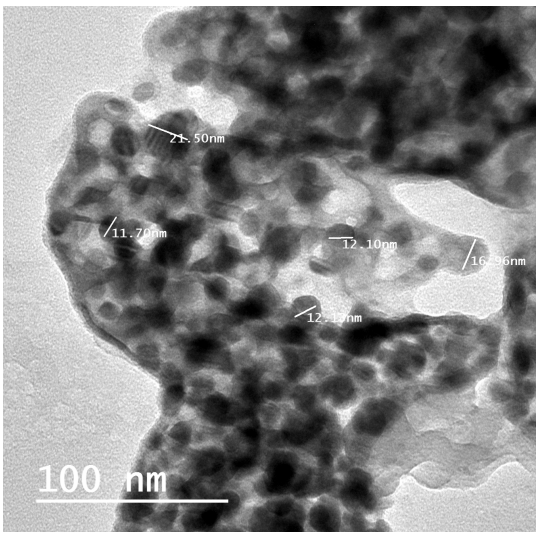

x = 0

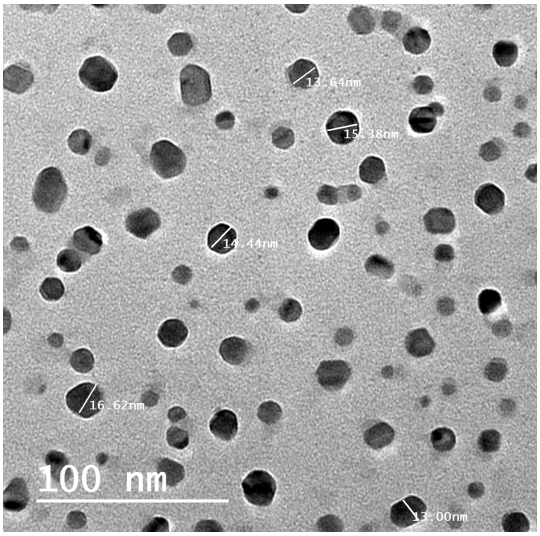

x = 0.1

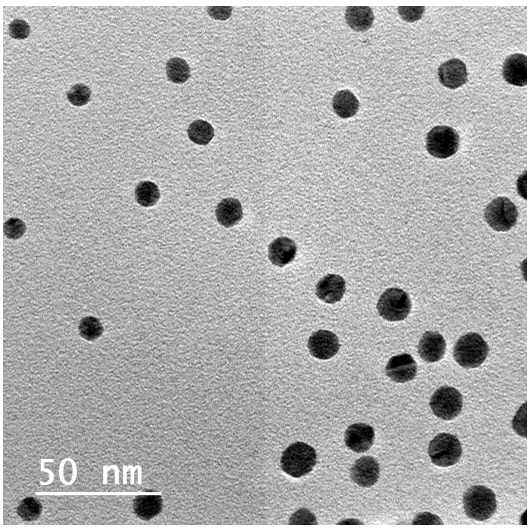

x = 0.2

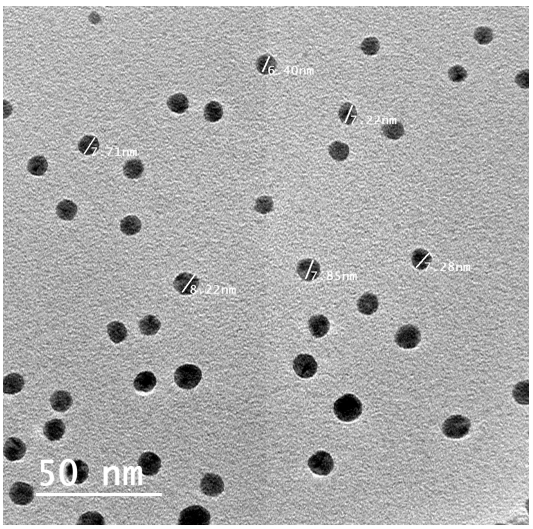

x = 0.3

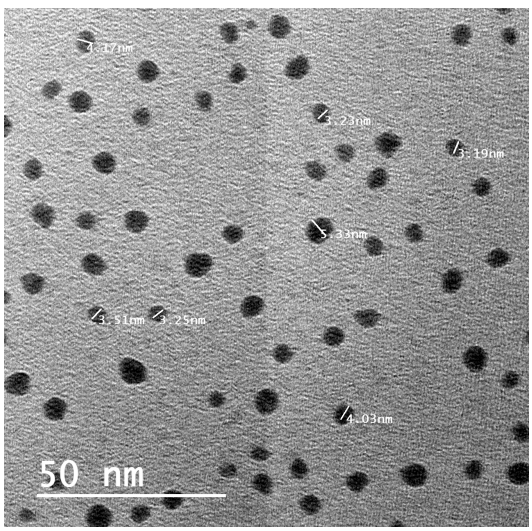

x = 0.4

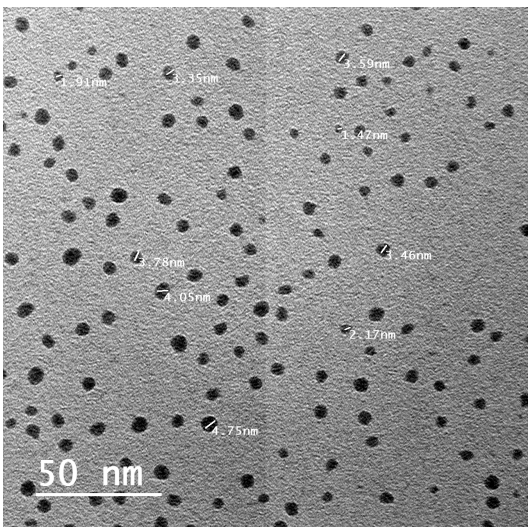

x = 0.5

(a)

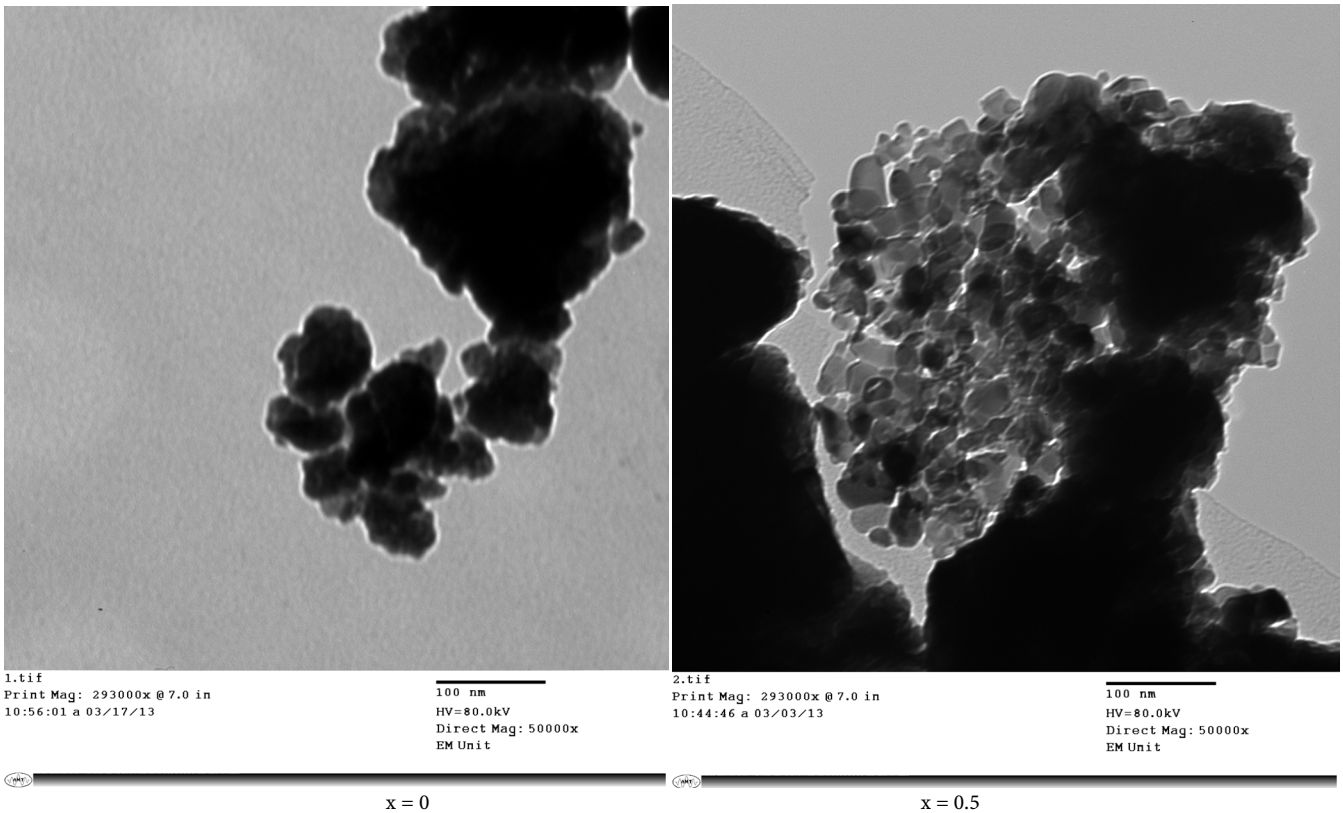

x = 0 x = 0.5

(b)

Figure 10. TEM for $Pb_{1-x}Ni_xTiO_3$. (a) co-precipitation samples, (b) ceramic samples.

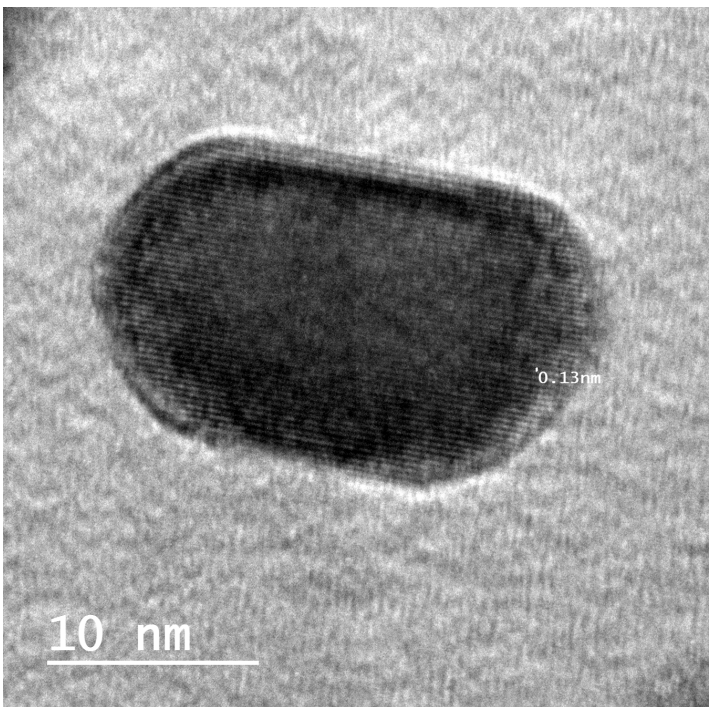

Figure 11. TEM micrograph showing $Pb_{0.5}Ni_{0.5}TiO_3$ nanocrystal.

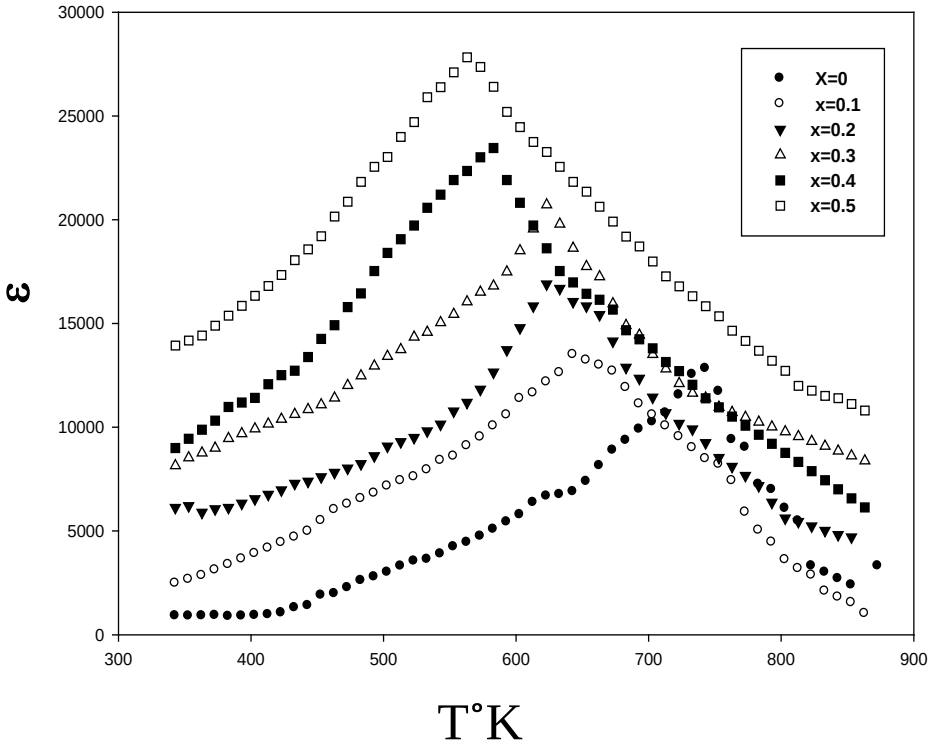

(a)

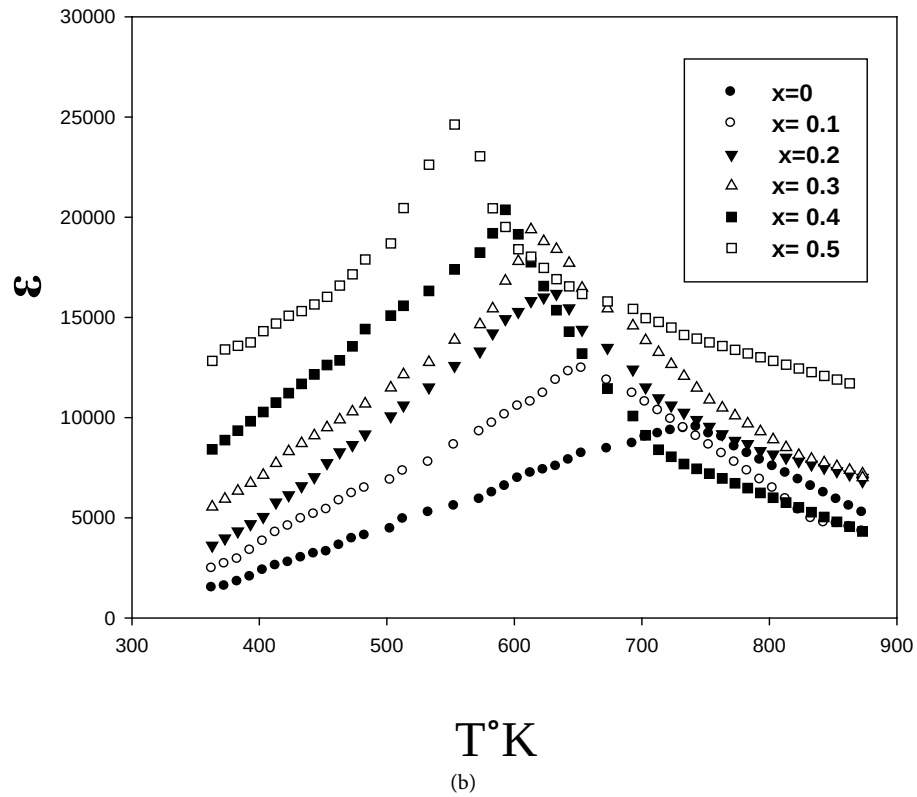

(b)

Figure 12. The dielectric constant (έ) for $Pb_{1-x}Ni_xTiO_3$ system vs. T K for (a) co-precipitation method and (b) ceramic method.

The samples have a first order phase transition from tetragonal to cubic phase at certain curie temperature T_c. The material converted from ferroelectric to Para electric state. The variation of curie temperature T_c and the value of dielectric constant are shown in the Figure 13. The behavior of ε identifies that our samples are nonrelaxor. Maximum ε at T_c are achieved in pure and Ni content samples increasing the Ni concentration increase the value of dielectric constant where T_c is shifted to lower temperature. The ε shows weak temperature dependents in the temperature rang (300 - 450 ˚k) for all samples. This range shifts to lower temperature by increasing Ni content. The presence of ferroelectric to paraelectric phase transition peaks of ε in the temperature range (560 - 700 ˚k) are clearly seen in Figure 12 which is an evidence for the existence of ferroelectricity for all fabricated ceramic and co-precipitation samples. It is also shown from Figure 12 that the value of ε for samples prepared by co-precipitation method is higher than samples prepared by ceramic method. It may be recognized to the fact that the decrease in grain size leads to the increase of dielectric constant [18]. This can be attributed to the fact that as the grain size increases the grain boundaries get smaller and clamp the domain wall to some extent.

It is clearly depicted that all the dielectric constant show a distinct phase transition point characterized by narrow curie peak, Which may be due to the absence of heterogeneity [19]. The dielectric constant increase by increasing Ni contents due to the increase of space charge contribution [20]. The dielectric constant is increased by increasing temperature, but is nearly independent of frequency especially in the vicinity of the phase transition temperature. The dielectric constant peak at the transition temperature systematically increase as the grain size decrease for both systems prepared by ceramic and co-precipitation methods, however there is a decrease in T_c with decreasing grain size for both systems, which is consistent with the observation [9]. All compositions show narrow peak in dielectric constant which indicate sharp phase transition.

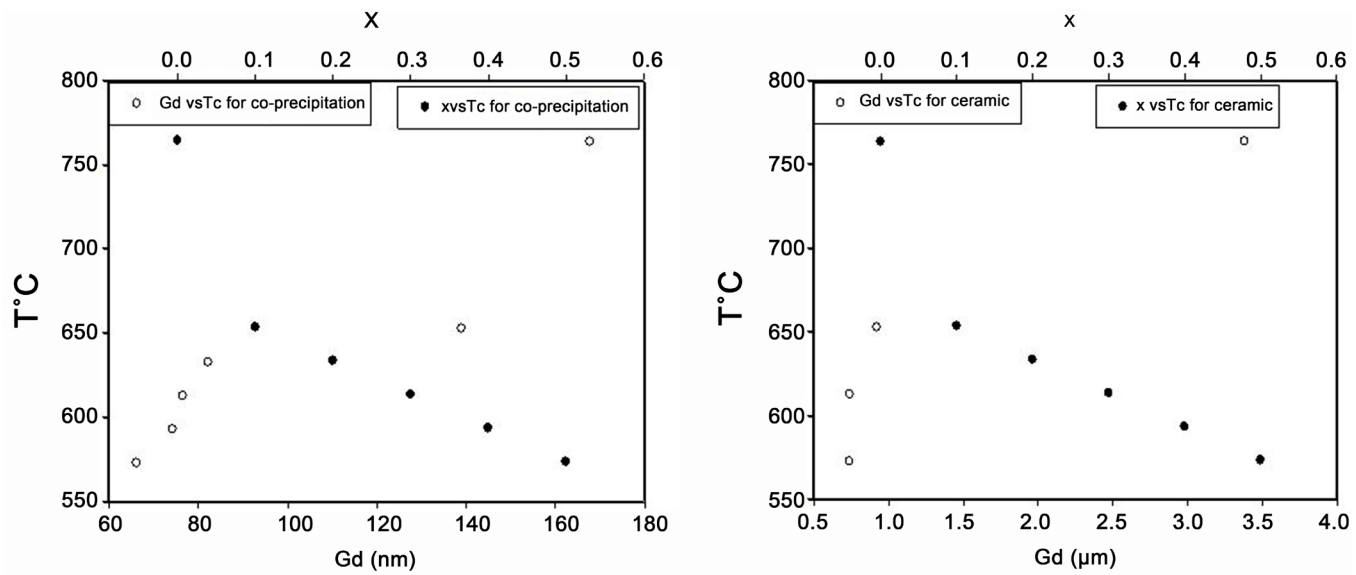

Figure 13. Grain-size dependence of curie constants for co-precipitation and ceramic methods.

4. Conclusion

The XRD patterns contain single phase, $PbTiO_3$ phase. Around $2\theta = 31.46$ splitted peak (001/100) is observed, indicating the presence of tetragonal phase. The studies of IR spectroscopy confirm the formation of a perovskite structure. The $PbTiO_3$ powder derived from ceramic method consists of particles with grain size ranged from 3.3 to 0.7 μm. The SEM of co-precipitation samples shows that the microstructure is very dense. The variation of the grain size of both samples as a function of Ni content showed a decrease in grain size where the grain size for co-precipitation samples ranged from 167.76 to 66.22 nm. The TEM images show small ferroelectric crystallite size about 14 to 3 nm for the co-precipitation samples and from 48 to 26 nm for the ceramic samples. The dielectric constant is increased by increasing temperature, but is nearly independent of frequency. The behavior of ε identifies that our samples are non-relaxor. Increasing the Ni concentration increases the value of dielectric constant and the T_c is shifted to lower temperature.

References

[1] Amarande, L., Miclea, C., Cioangher, M., Grecu, M.N., Pasuk, I. and Negrea, R.F. (2014) Influence of Co-Dopants Average Valence on Microstructural and Electromechanical Properties of Lead Titanate Ceramics. *Journal of the European Ceramic Society*, **34**, 1191-1200. http://dx.doi.org/10.1016/j.jeurceramsoc.2013.12.002

[2] Nagarbawadi, M.A., Jangade, P.S. and Bagwan, S.T. (2014) The Influence of Calcium Doping on Structural and Electrical Properties of Ferroelectric Lead Titanate Ceramic. *IOSR Journal of Applied Physics* (*IOSR-JAP*), **6**, 15-19. http://dx.doi.org/10.9790/4861-06321519

[3] Shi, L., Liao, Q., Zhang, B., Zhang, J. and Guo, D. (2014) Structure and Electrical Properties of $(1-x)(0.1BiYbO_3 - 0.9PbTiO_3) - xPb(Zn_{1/3}Nb_{2/3})O_3$ High-Temperature Ternary Piezoelectric Ceramics. *Materials Letters*, **114**, 100-102. http://dx.doi.org/10.1016/j.matlet.2013.09.061

[4] Gupta, R., Verma, S., Singh, V. and Bamzai, K.K. (2015) Preparation, Structural, Electrical, and Ferroelectric Properties of Lead Niobate-Lead Zirconate-Lead Titanate Ternary System. *Journal of Ceramics*, **2015**, Article ID: 835150.

[5] Tartaj, J., Moure, C., Lascano, L. and Duran, P. (2001) Sintering of Dense Ceramics Bodies of Pure Lead Titanate Obtained by Seeding-Assisted Chemical Sol-Gel. *Materials Research Bulletin*, **36**, 2301-2310. http://dx.doi.org/10.1016/S0025-5408(01)00712-7

[6] Yanaka, E., Watenabe, H., Kimura, N., Kanaya, N. and Ohkuma, H. (1988) Structural, Ferroelectric and Pyroelectric Properties of Highly c Axis Oriented P1-xCaxTiO$_3$ Thin Films Grown by Radio-Frequency Magentron Sputtring. *Journal of Vacuum Science & Technology A*: *Vacuum*, *Surfaces*, *Films*, **6**, 2921–2928. http://dx.doi.org/10.1116/1.575452

[7] Mitoseriu, L., Ciomaga, C.E., Buscaglia, V., Stoleriu, L., Piazza, D., *et al.* (2007) Hysteresis and Tunability Characteristics of $Ba(Zr,Ti)O_3$ Ceramics Described by First Order Reversal Curves Diagrams. *Journal of the European Ceramic Society*, **27**, 3723-3726. http://dx.doi.org/10.1016/j.jeurceramsoc.2007.02.085

[8] Arlt, G. (1990) Twinning in Ferroelectric and Ferroelastic Ceramics: Stress Relief. *Journal of Materials Science*, **25**, 2655-2666. http://dx.doi.org/10.1007/BF00584864

[9] Randall, C.A., Kim, N., Kucera, J.-P., Cao, W.W. and Shrout, T.R. (1998) Intrinsic and Extrinsic Size Effects in Fine-Grained Morphotropic-Phase-Boundary Lead Zirconate Titanate

Ceramics. *Journal of the American Ceramic Society*, **81**, 677-688. http://dx.doi.org/10.1111/j.1151-2916.1998.tb02389.x

[10] Arlt, G., Hennings, D. and de With, G. (1985) Dielectric Properties of Fine-Grained Barium Titanate Ceramics. *Journal of Applied Physics*, **58**, 1619-1625. http://dx.doi.org/10.1063/1.336051

[11] Hsiang, H.-I. and Yen, F.-S. (1996) Effect of Crystallite Size on the Ferroelectric Domain Growth of Ultrafine $BaTiO_3$ Powders. *Journal of the American Ceramic Society*, **79**, 1053-1060. http://dx.doi.org/10.1111/j.1151-2916.1996.tb08547.x

[12] Cho, S.B., Oledzka, M. and Riman, R.E. (2001) Hydrothermal Synthesis of Acicular Lead Zirconate Titanate (PZT). *Journal of Crystal Growth*, **226**, 313-326. http://dx.doi.org/10.1016/S0022-0248(01)00857-0

[13] Hu, J., Chen, G.H. and Lo, I.M.C. (2005) Removal and Recovery of Cr(VI) from Wastewater by Maghemite Nanoparticles. *Water Research*, **39**, 4528-4538. http://dx.doi.org/10.1016/j.watres.2005.05.051

[14] Sun, J., Zhuo, S.B., Hou, P., Yang, Y., Weng, J., Li, X.H. and Li, M.Y. (2007) Synthesis and Characterization of Biocompatible Fe_3O_4 Nanoparticles. *Journal of Biomedical Materials Research Part A*, **80A**, 333-341. http://dx.doi.org/10.1002/jbm.a.30909

[15] Kong, L.B., Ma, J., Zhang, R.F., Zhu, W. and Tan, O.K. (2002) Lead Zirconate Titanate Ceramics Achieved by Reaction Sintering of PbO and High-Energy Ball Milled $(ZrTi)O_2$ Nanosized Powders. *Materials Letters*, **55**, 370-377. http://dx.doi.org/10.1016/S0167-577X(02)00395-6

[16] Atkin, R.B. and Fulrath, R.M. (1971) Point Defects and Sintering of Lead Zirconate-Titanate. *Journal of the American Ceramic Society*, **54**, 265-270. http://dx.doi.org/10.1111/j.1151-2916.1971.tb12286.x

[17] Tung, V.T., Tinh, N.T., Yen, N.H. and Tuan, D.A. (2013) Evaluation of Electromechanical Coupling Factor for Piezoelectric Materials Using Finite Element Modeling. *International Journal of Materials and Chemistry*, **3**, 59-63.

[18] Kumari, N., Singh, A. and Manda, J. (2013) Lead Zirconate Titanate Piezoelectric Ceramics with Nickel Oxide Additions. *International Refereed Journal of Engineering and Science*, **2**, 51-55.

[19] Gupta, R., Verma, S., Singh, D., Singh, K. and Bamzai, K. (2015) Effect of Ni/Nb on Structure, Electrical and Ferroelectric Properties of 0.5PNN-0.5PZT Ceramics. *Processing and Application of Ceramics*, **9**, 1-9. http://dx.doi.org/10.2298/PAC1501001G

[20] Gupa, V., Bamzai, K.K., Kotru, P.N. and Wanklyn, B.M. (2006) Dielectric Properties, AC Conductivity and Thermal Behaviour of Flux Grown Cadmium Titanate Crystals. *Materials Science and Engineering*: *B*, **130**, 163-172. http://dx.doi.org/10.1016/j.mseb.2006.03.006

Scientific Research Publishing

Submit or recommend next manuscript to SCIRP and we will provide best service for you:

Accepting pre-submission inquiries through Email, Facebook, LinkedIn, Twitter, etc.
A wide selection of journals (inclusive of 9 subjects, more than 200 journals)
Providing 24-hour high-quality service
User-friendly online submission system
Fair and swift peer-review system
Efficient typesetting and proofreading procedure
Display of the result of downloads and visits, as well as the number of cited articles
Maximum dissemination of your research work

Submit your manuscript at: http://papersubmission.scirp.org/
Or contact ojapps@scirp.org